

A CHARACTERISATION OF THE HOFFMAN-WOHLGEMUTH SURFACES IN TERMS OF THEIR SYMMETRIES

PINIO SIMÕES & VALÉRIO RAMOS BATISTA

Abstract

For an embedded singly periodic minimal surface \tilde{M} with genus $g \geq 4$ and annular ends, some weak symmetry hypotheses imply its congruence with one of the Hoffman-Wohlgemuth examples. We give a very geometrical proof of this fact, along which they come out many valuable clues for the understanding of these surfaces.

1. Introduction

The beauty of a characterisation theorem resides particularly in its demonstration, where a lot of intrinsic and fascinating properties are revealed. For complete embedded minimal surfaces of finite total curvature in the euclidean space $\mathbb{E} = \mathbb{R}^3$, R.Schoen published a strong result in 1983: if S is such a surface, then it must be the catenoid providing it has exactly two ends (see [28]). Later in 1991, F.López and A.Ros proved that, if S has genus zero, then it is the catenoid or the flat plane (see [14]). Together, their works showed that other examples of S should have positive genera *and* more than two ends. Meanwhile, C.Costa characterised all minimal tori S with three ends (see [1]), but a torus S with four ends or more could not exist by the Hoffman-Meeks' conjecture that $\# \text{ ends} \leq \text{genus} + 2$. Higher genus examples can be found in [31].

In 1990, D.Hoffman and W.Meeks gave examples of S with three ends and arbitrary positive genus, which in 1995 were generalised by D.Hoffman and H.Karcher (see [9] and [7]). Under symmetry hypothesis, in 2001 F.Martín and M.Weber classified them (see [17]). One year later, M.Traizet replaced the symmetry hypothesis by the weaker concept of *configuration* and got a characterisation of the Hoffman-Karcher two-parameter family (see [29]). Moreover, in the same work he gave examples of totally asymmetric S , answering the open question from [7, sec 5.2].

Traizet's surfaces have high fixed genus, 5 ends and can assume different configurations. They show that any classification result of S will need more constraints, for instance, a fixed conformal structure. However, in [27] it is shown that, when self-intersections are allowed at the ends of S , the conformal structure, even together with symmetry constraint, is insufficient to characterise the surface.

After having discussed S in $\mathbb{E} = \mathbb{R}^3$, it is important to mention the advances in $\mathbb{E} = \mathbb{R}^3/\mathcal{T}$, where \mathcal{T} is a cyclic translation group. If S is a torus with a finite number of planar ends, then S belongs to Riemann's family according to [19]. The genus-one hypothesis is necessary because of an unpublished work from F.Weier, *Adding handles to the Riemann examples*. However, further characterisation results had to impose more constraints to be accomplished. In 1997 and 2000, the beautiful works [15], [16] from F.Martín and D.Rodríguez showed that mild hypotheses on ends, genus and symmetries imply that S is one of the Callahan-Hoffman-Meeks' examples [3]. The symmetry conditions are necessary due to a work from M.Callahan,

D.Hoffman and H.Karcher (see [2]). For results on S with helicoidal and Scherk-ends, see [20] and [25].

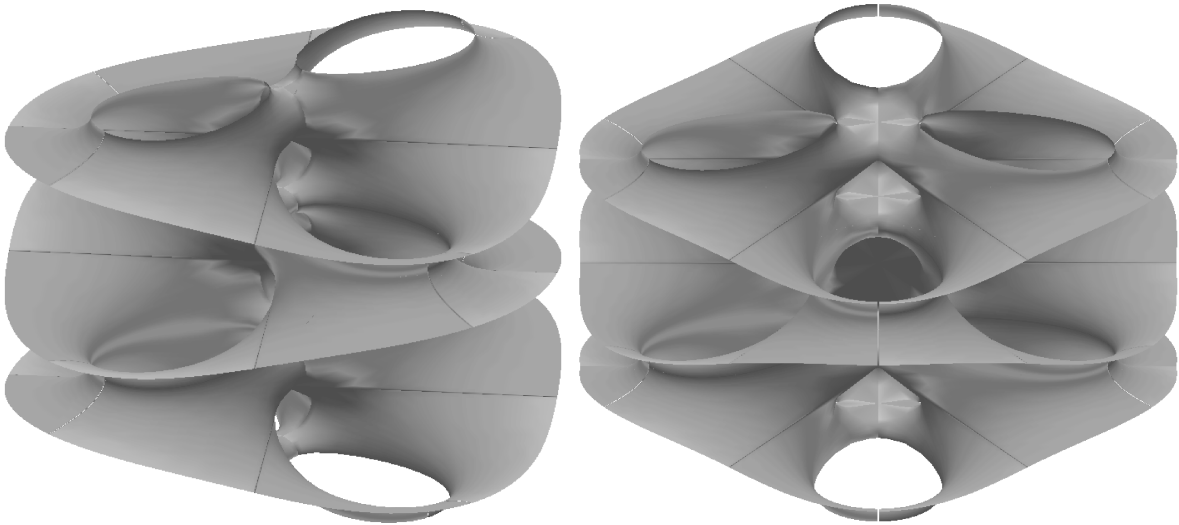


Figure 1: The Hoffman-Wohlgemuth surfaces of genera 5 and 9.

If S is doubly periodic, the reader will find beautiful works like [12] and [24]. Back to the singly periodic case for S with annular ends, our attention will now focus on the unpublished work from D.Hoffman and M.Wohlgemuth, *New embedded minimal surfaces of Riemann type*. These surfaces were obtained by adding Noevius handles to the examples in [3]. Of course, the sole addition of handles is by itself of little interest nowadays, except in the case of general results as [11]. Therefore, a characterisation theorem brings much more of new and good knowledge, particularly in the case of the Hoffman-Wohlgemuth surfaces. This present work is strongly inspired in the beautiful ideas of [16], but there are substantial differences, mainly because they deal with one-dimensional period problems, whereas the periods are two-dimensional in our case. In their work, the first part uses genus, ends and symmetry hypotheses to get Weierstrass data, and these allow 3 different family of surfaces. In the second part, hard computations of elliptic integrals finally show that just one family admits an embedded member, and only one, for any fixed odd genus starting from 3.

Our first part is similar to theirs, but from the Weierstrass data (g, dh) one gets 32 different families. However, simple geometric arguments quickly drop this number to 4. In the second part, a very basic handling of $\int g dh$ and $\int dh/g$ shows that, on 3 of the cases, the period is always open on a suitable closed curve. This is quite unexpected for two-dimensional problems, where non-existence in general follows from periods that can be separately solved, and then it lacks a *simultaneous* solution. Moreover, in our cases neither $\int g dh$ nor $\int dh/g$ will need any *explicit* formulation.

The fact that one of the periods never closes is apparently due to the presence of a ‘‘Gaussian geodesic’’. By this concept we mean a planar curve of reflectional symmetry, which is the graph of an even real-analytic function $f : \mathbb{R} \rightarrow (0, 1]$, where $f(0) = 1$, $f' \neq 0$

in \mathbb{R}^* and $\lim_{x \rightarrow \infty} f(x) = 0$. Since 1997, when the second author started his doctoral studies in Germany, he observed that they failed all construction attempts of minimal surfaces containing a Gaussian geodesic. In total one tried 15 different examples and periods never closed. The same held for “inverted Gaussians”, now with odd $f : \mathbb{R} \rightarrow (-1, 1)$, $f' = 0$ only at 0 and $\lim_{x \rightarrow +\infty} f(x) = 1$.

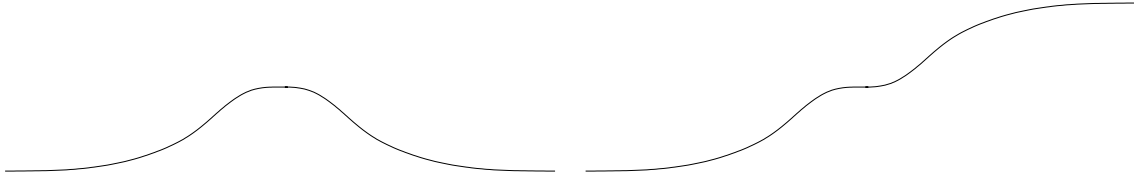


Figure 2: A standard and an inverted Gaussian.

Hitherto, it remains open the question whether an S with Gaussian geodesic exists. However, Section 6 of this present work might bring some good ideas for a future study of this question. At last, the closure of periods succeeds for the Hoffman-Wohlgemuth surfaces, and yet the proof *is* easy (see Section 7). However, a *unique* solution could only be verified with numerical computation. This is typical for two-dimensional problems involving no López-Ros parameter, for till nowadays there is *just one* formal uniqueness demonstration of this kind, recently achieved by L.Ferrer and F.Martín (see [6]). Moreover, the proof in [6] is very laborious and reports a surface found 6 years beforehand (see [8]). Our result must be then interpreted in the sense that the Hoffman-Wohlgemuth family might occasionally admit two or more members with the same genus.

We shall give now a definition concerning *ends* of a complete Riemannian surface:

Definition 1.1. Consider a complete Riemannian surface R and a sequence of enclosed compact balls $B_n \subset R$, $n \in \mathbb{N}$, with $\cup_{n=0}^{\infty} B_n = R$. Suppose there is $n_0 > 0$ and a connected component \mathcal{E} of $R \setminus B_{n_0}$ such that $\mathcal{E} \setminus B_m$ and $\mathcal{E} \setminus B_n$ are homeomorphic for any $m, n \geq n_0$. In this case one has an equivalence relation $\mathcal{E} \setminus B_m \sim \mathcal{E} \setminus B_n$ and the corresponding equivalence class is called an *end* of S . We also denote any of this class representative by \mathcal{E} .

Now we present the main theorem of this paper:

Theorem 1.1. Let \tilde{M} be a properly embedded minimal surface in \mathbb{R}^3 such that

- i) \tilde{M} has an infinite number of annular ends;
- ii) \tilde{M} is invariant under a cyclic group of screw motions \mathcal{T}_θ ;
- iii) $\tilde{M}/\mathcal{T}_\theta$ has genus $\varrho \geq 4$ and exactly two ends;
- iv) $|\text{Iso}(\tilde{M}/\mathcal{T}_\theta)| \geq 2(\varrho + 3)$;
- v) \exists a conformal generator $\sigma \in \text{Iso}(\tilde{M}/\mathcal{T}_\theta)$, and $r_1, r_2 \in \tilde{M}$ such that $\sigma(r_i) \neq r_i \notin \{r_j, \sigma(r_j)\} = \sigma(\{r_j, \sigma(r_j)\})$, for $\{i, j\} = \{1, 2\}$.

Then $(\varrho + 1)/2$ is odd and \tilde{M} is the Hoffman-Wohlgemuth surface M_ϱ of genus ϱ .

REMARKS: M_ϱ exists only for $\varrho = 4k + 1$, $k \in \mathbb{N}^*$, as we shall see in Sections 3 and 7. Although apparently excessive, hypothesis (v) is necessary. Indeed, all surfaces from Callahan-Hoffman-Meeks of genus $\varrho > 3$ verify (i)-(iv), but not (v). It could be replaced

by “ $\text{Iso}(\tilde{M}/\mathcal{T}) < 4(\rho + 1)$ ”, but in the praxis upper bounds for isometry groups are hard to compute. By a “screw motion” we mean a rotation about an axis followed by a translation *not necessarily* in the axis direction.

The present work was supported by FAPESP grant number 05/00026-3.

2. Preliminaries

In this section we state some basic definitions and theorems. Throughout this work, surfaces are considered connected and regular. Details can be found in [10], [13], [21] and [23].

Theorem 2.1. *Let $X : R \rightarrow \mathbb{E}$ be a complete isometric immersion of a Riemannian surface R into a three-dimensional complete flat space \mathbb{E} . If X is minimal and the total Gaussian curvature $\int_R K dA$ is finite, then R is biholomorphic to a compact Riemann surface \bar{R} punched at a finite number of points.*

Theorem 2.2. (Weierstrass representation). *Let R be a Riemann surface, g and dh meromorphic function and 1-differential form on R , such that the zeros of dh coincide with the poles and zeros of g . Suppose that $X : R \rightarrow \mathbb{E}$, given by*

$$X(p) := \text{Re} \int^p (\phi_1, \phi_2, \phi_3), \quad \text{where} \quad (\phi_1, \phi_2, \phi_3) := \frac{1}{2}(g^{-1} - g, ig^{-1} + ig, 2)dh, \quad (1)$$

is well-defined. Then X is a conformal minimal immersion. Conversely, every conformal minimal immersion $X : R \rightarrow \mathbb{E}$ can be expressed as (1) for some meromorphic function g and 1-form dh .

Definition 2.1. The pair (g, dh) is the *Weierstrass data* and ϕ_1, ϕ_2, ϕ_3 are the *Weierstrass forms* on R of the minimal immersion $X : R \rightarrow X(R) \subset \mathbb{E}$.

Theorem 2.3. *Under the hypotheses of Theorems 2.1 and 2.2, the Weierstrass data (g, dh) extend meromorphically on \bar{R} .*

Theorem 2.4. (Callahan-Hoffman-Meeks [4]). *Suppose $X : R \rightarrow \mathbb{R}^3$ is a proper minimal embedding with more than one end. If $X(R)$ has an infinite group of symmetries, then it is either a catenoid or has the following properties:*

1. $\# \text{ends}(X(R)) = \infty$;
2. there is a screw motion \mathcal{T}_θ in \mathbb{R}^3 such that $\mathcal{T}_\theta(X(R)) = X(R)$;
3. all annular ends of $X(R)$ are flat;
4. the total curvature of $S := X(R)/\mathcal{T}_\theta$ is finite if, and only if $\pi_1(S)$ is finitely generated. In this case $\int_S K dA = 2\pi[\chi(S) - \# \text{ends}(S)]$.

The function g is the stereographic projection of the Gauß map $N : R \rightarrow S^2$ of the minimal immersion X . It is a covering map of $\hat{\mathbb{C}}$ and $\int_S K dA = -4\pi \text{deg}(g)$. These facts will be largely used throughout this work.

3. The Weierstrass data of \tilde{M}

Considering the hypotheses (i) and (iii) of Theorem 1.1, at least one end of $\tilde{M}/\mathcal{T}_\theta$ must be an annulus in \mathbb{R}^3 . Since \tilde{M} is proper, the other end must be unbounded, and also an annulus because \tilde{M} is embedded. Therefore, all ends of \tilde{M} are annular and hence flat by Theorem 2.4. Now we apply (iii) to Theorem 2.4 and conclude that $\tilde{M}/\mathcal{T}_\theta$ has total curvature $-4\pi(\varrho + 1)$. From Theorem 2.1 it follows that $\tilde{M}/\mathcal{T}_\theta$ is biholomorphic to a compact Riemann surface \overline{M} punched at two points, because of (iii). We call them p_1 and p_2 .

Now define $M := \overline{M} \setminus \{p_1, p_2\}$. From the converse of Theorem 2.2, we have on M a Weierstrass pair (g, dh) which extends meromorphically on \overline{M} by Theorem 2.3. Notice that $\deg(g) = \varrho + 1$. Up to a rigid motion in \mathbb{R}^3 , $g(p_1) = 0$ and so $g(p_2) = \infty$ because of *Alexander duality*. Let us write $\mathcal{T}_\theta = \rho \circ \tau$, where ρ is a rotation about Ox_3 and τ a translation. The same arguments from [15, p187-8] easily generalise for non-vertical τ , and they imply that \tilde{M} is invariant under $\tau := \tau^2$, whence also invariant under $\rho := \rho^2$. If $\mathbf{s} = \rho \circ \tau$ and $m = \text{ord}(\rho)$, then both $\tilde{M}/\langle \tau \rangle$ and $\tilde{M}/\langle \mathbf{s} \rangle$ will have the same total curvature, since each of them is an m -sheeted branched covering of $\tilde{M}/\langle \rho, \tau \rangle$.

ASSERTION 1: $|Iso(\tilde{M}/\langle \tau \rangle)| \geq |Iso(\tilde{M}/\langle \mathbf{s} \rangle)|$.

Proof. We have $\tau = \rho^{m-1} \circ \mathbf{s}$. Hence the map $\langle \rho \rangle \rightarrow \langle \rho, \mathbf{s} \rangle / \langle \tau \rangle$, given by $\rho^i \mapsto \rho^i \langle \tau \rangle$, is an isomorphism. Therefore, $|\langle \rho, \mathbf{s} \rangle / \langle \tau \rangle| = m$. If $G = Iso(\tilde{M})$, then

$$\left| \frac{G}{\langle \rho, \mathbf{s} \rangle} \right| \cdot \left| \frac{\langle \rho, \mathbf{s} \rangle}{\langle \tau \rangle} \right| = \left| \frac{G}{\langle \tau \rangle} \right|.$$

The map $\langle \rho \rangle \rightarrow \langle \rho, \mathbf{s} \rangle / \langle \mathbf{s} \rangle$, given by $\rho^i \mapsto \rho^i \langle \mathbf{s} \rangle$, is an epimorphism. Therefore, $|\langle \rho, \mathbf{s} \rangle / \langle \mathbf{s} \rangle| \leq m$. Now

$$\left| \frac{G}{\langle \rho, \mathbf{s} \rangle} \right| \cdot \left| \frac{\langle \rho, \mathbf{s} \rangle}{\langle \mathbf{s} \rangle} \right| = \left| \frac{G}{\langle \mathbf{s} \rangle} \right|,$$

whence $|G/\langle \mathbf{s} \rangle| \leq |G/\langle \tau \rangle|$.

q.e.d.

Precisely CLAIM 3 of [15, p189] implies that τ is vertical. By following the same ideas as in [15, p189-0], one sees that \tilde{M} is invariant under $\mathcal{T}_\theta^{-1} \circ \tau \circ \mathcal{T}_\theta = \tau$. Now the previous arguments apply for ρ, τ and \mathcal{T}_θ in the place of ρ, τ and \mathbf{s} , respectively. Therefore, we can rewrite Theorem 1.1 as follows:

Theorem 3.1. *Let \tilde{M} be a properly embedded minimal surface in \mathbb{R}^3 such that*

- i) \tilde{M} has an infinite number of annular ends;
- ii) \tilde{M} is invariant under a cyclic group of vertical translations $\mathcal{T} = \langle \tau \rangle$;
- iii) \tilde{M}/\mathcal{T} has genus $\varrho \geq 4$ and exactly two ends;
- iv) $|Iso(\tilde{M}/\mathcal{T})| \geq 2(\varrho + 3)$;
- v) \exists a conformal generator $\sigma \in Iso(\tilde{M}/\mathcal{T})$, and $r_1, r_2 \in \tilde{M}$ such that $\sigma(r_i) \neq r_i \notin \{r_j, \sigma(r_j)\} = \sigma(\{r_j, \sigma(r_j)\})$, for $\{i, j\} = \{1, 2\}$.

Then $(\varrho + 1)/2$ is odd and \tilde{M} is the Hoffman-Wohlgemuth surface M_ϱ of genus ϱ .

At this point, we re-define $M := \tilde{M}/\mathcal{T}$, $\overline{M} := M \cup \{p_1, p_2\}$ and (g, dh) on \overline{M} given by Theorem 2.3. Now the same arguments from [16, p448] firstly imply that the group Δ of automorphisms of \overline{M} has a cyclic subgroup $\mathcal{G} := \{A \in \Delta : A \text{ is holomorphic and } A(p_1) = p_1\}$. Secondly, if J is a generator of \mathcal{G} , there is a corresponding symmetry \tilde{J} of \tilde{M} which fixes a point in space. From (v) and the fact that \mathcal{G} is cyclic, we may take $J = \sigma$.

By Hurwitz's theorem Δ is finite, and so is \mathcal{G} . Therefore, $\text{ord}(\tilde{J})$ is finite and equals $\text{ord}(J) = n$. Without loss of generality we consider $\tilde{J}(0, 0, 0) = (0, 0, 0)$. The rigidity of \tilde{M} (see [5]) and the fact that \tilde{J} has a discrete fixed-point set on \tilde{M} (possibly empty) imply that \tilde{J} keeps fixed the vertical x_3 -axis. Since $[\Delta : \mathcal{G}] \leq 4$, from (iv) we have $n \geq (\varrho + 3)/2$, $\varrho \geq 4$. From [15, p189], \tilde{J} is a $2\pi/n$ -rotation around Ox_3 composed with a reflection in Ox_1x_2 . Up to a homothety, $\tau(x) = x + (0, 0, 2)$.

As in [16, p449], one defines for $q \in \overline{M}$ the stabiliser $S_q = \{f \in \mathcal{G} : f(q) = q\}$ and the orbit $O_q = \{q, J(q), \dots, J^{n-1}(q)\}$. Since $n = \#O_q \cdot \#S_q$, the Riemann-Hurwitz formula for the branched covering $\zeta : \overline{M} \rightarrow \overline{M}/J$ gives

$$n \cdot \chi(\overline{M}/J) = \chi(\overline{M}) + \left(2n - 2 + \sum_{q \in \overline{M}} (\#S_q - 1) \right). \quad (2)$$

In (2) the term $2n - 2$ corresponds to $p_{1,2}$. For each q with $\#S_q > 1$, consider the set $O_q = O_{J(q)} = \dots = O_{J^{n-1}(q)}$. There are exactly s disjoint sets like that, $s \in \mathbb{N}^*$, and for each set we call its cardinality m_i , $i = 1, \dots, s$. One rewrites (2) as follows:

$$n \cdot \chi(\overline{M}/J) = 2n - 2\varrho + \sum_{i=1}^s (n - m_i). \quad (3)$$

Up to re-indexing, from (v) we have $m_1 = m_2 = 2$ and $s \geq 2$. Since $2n - \varrho \geq 3$, one guarantees that $\chi(\overline{M}/J) \geq 2/n > 0$. Therefore, \overline{M}/J is the Riemann sphere with Euler characteristic 2. Hence (3) simplifies to

$$\sum_{i=1}^s (n - m_i) = 2\varrho. \quad (4)$$

Since \tilde{J}^2 is a rotation around Ox_3 , we conclude that $m_i \leq 2$, $\forall i$. For a minimal surface invariant under a rotation \mathcal{R} about Ox_3 , in [3] one proves that any flat horizontal end will have an order of pole (or zero) for g given by $j \cdot \text{ord}(\mathcal{R}) + 1$, where j is a certain positive integer. Moreover, any regular point with vertical normal will have an order of pole (or zero) for g given by $j \cdot \text{ord}(\mathcal{R}) - 1$. Hence $\text{ord}_{p_i}(g) \geq n/2 + 1$ and $\text{ord}_{r_i}(g) \geq n/2 - 1$. For $s = 2$, it follows from (4) that $n = 2 + \varrho$. Hence $\text{deg}(g) \geq 1 + \varrho/2 + 1 + 2(1 + \varrho/2 - 1)$, contradicting $\text{deg}(g) = \varrho + 1$. Thus $s \geq 3$.

ASSERTION 2: $n = (\varrho + 3)/2$.

Proof. If one had $n > (\varrho + 3)/2$, from the above arguments it would follow that

$$\text{deg}(g) > \frac{\varrho + 3}{4} + 1 + 3 \left(\frac{\varrho + 3}{4} - 1 \right).$$

Hence $\deg(g) > \varrho + 1$, a contradiction. Therefore $n = (\varrho + 3)/2$. q.e.d.

On the one hand, it follows now by (4) that $s = 3$ implies $m_3 = (1 - \varrho)/2 \notin \{1, 2\}$, a contradiction. Hence $s \geq 4$. On the other hand, $s \geq 6$ gives $\varrho + 5 \leq m_3 + m_4 + m_5 + m_6$. Since $\varrho \geq 4$ and $m_i \leq 2, \forall i$, this is once again a contradiction. Therefore $4 \leq s \leq 5$. From now on we write $\varrho = 4k + 1, n = 2(k + 1)$ and so $\deg(g) = 2(2k + 1)$, for $k \in \mathbb{N}^*$.

If $s = 5$, then $k = 1$ and so $m_3 = m_4 = m_5 = 2, \deg(g) = 6$. This means that M has exactly ten points where the normal is vertical. Since $\text{ord}(J^2) = 2$, then four points of M contribute each with at least 1 for $\deg(g)$, while $\text{ord}_{p_i}(g) \geq 3, i = 1, 2$. Hence $\deg(g) \geq 4 + 3 > 6$, which is absurd. Consequently, $s = 4$.

Now (4) simplifies to

$$\sum_{i=3}^4 (2(k+1) - m_i) = 4k + 2, \quad (5)$$

whence $m_3 = m_4 = 1$. Then each fundamental piece of \tilde{M} has eight points with vertical normal vectors: two ends $\{p_1, p_2\}$, two points on Ox_3 with $m_3 = m_4 = 1$ that we call $\{q_1, q_2\}$, and four points $r_i, i = 1, \dots, 4$, corresponding to $m_1 = m_2 = 2$. Notice that $\deg(g) = 2(2k + 1)$.

Since $\sigma = J$ and \tilde{J} is a rigid motion, we conclude that $g(r_i) = g(\sigma(r_i)), \forall i$. Now it is clear that $g(q_1) = 1/g(q_2)$. With no loss of generality we take $r_3 = \sigma(r_1), r_4 = \sigma(r_2), g(p_1) = g(q_2) = g(r_{1,3}) = 0$ and $g(p_2) = g(q_1) = g(r_{2,4}) = \infty$. Hence, the divisor of g is written as

$$[g] = \frac{p_1^{k+2}(q_2 r_1 r_3)^k}{p_2^{k+2}(q_1 r_2 r_4)^k}. \quad (6)$$

Now we are going to write down the divisor of dh . For the minimal immersion $X : \tilde{M} \rightarrow \mathbb{R}^3/\mathcal{T}$, determined by (g, dh) , at each point where g is vertical we must have a zero for dh , exactly of the same order as g . Moreover, dh must have zeros at the ends $p_{1,2}$ both of order $-2 + \text{ord}(g)_{p_{1,2}} = k$ (see [10, p26] for details). From (6) it follows that

$$[dh] = (p_1 p_2 q_1 q_2 r_1 r_2 r_3 r_4)^k. \quad (7)$$

We recall that \mathcal{T} is generated by the vertical translation $\tau(x) = x + (0, 0, 2)$. So we take a fundamental piece of \tilde{M} in the slab $\mathcal{S} := \{(x_1, x_2, x_3) \in \mathbb{R}^3 \mid -1 < x_3 \leq 1\}$ and the points $\tilde{q} \in \tilde{M}$ such that $\tilde{q}/\mathcal{T} \in \{q_1, q_2\}$. Since $J(q_i) = q_i$ and \tilde{J} is a rotation of $\pi/(k+1)$ around Ox_3 followed by a reflection in Ox_1x_2 , then any \tilde{q} is in Ox_3 . Among these points we have $\tilde{q}_{1,2}$ in \mathcal{S} . Therefore, $\tilde{J}(\tilde{q}_i) = (0, 0, 2n_i) - \tilde{q}_i$, for some $n_i \in \mathbb{Z}, i = 1, 2$. But \tilde{J} fixes $(0, 0, 0)$ and $\tilde{J}(\mathcal{S}) = \mathcal{S}$. We conclude that $\{\tilde{q}_1, \tilde{q}_2\} = \{(0, 0, 0), (0, 0, 1)\}$. Since $J(p_i) = p_i$, we also conclude that the planar ends $\tilde{p}_{1,2}$ of \tilde{M} are asymptotic to $x_3 = 0$ and $x_3 = 1$. We have settled $g(p_1) = 0$. Up to changing orientation of \tilde{M} , \tilde{p}_1 will correspond to $x_3 = 1$ and \tilde{p}_2 to $x_3 = 0$.

This means, given a symmetry which fixes one of the points p_i, q_i , it also fixes the others. Otherwise it interchanges $p_1 \leftrightarrow p_2$ and $q_1 \leftrightarrow q_2$. We saw already that \overline{M}/J is conformally \mathbb{C}^2 . Up to a Möbius transformation one can assume that

$$\zeta(p_1) = 0, \quad \zeta(p_2) = \infty \quad \text{and} \quad \zeta(q_1) = 1.$$

Therefore, $\zeta(q_2)$ equals a certain $s \in \mathbb{C} \setminus \{0, 1\}$, while $\zeta(r_{1,3}) = y_1$ and $\zeta(r_{2,4}) = y_2$, namely two distinct complex values in $\mathbb{C} \setminus \{0, 1, s\}$. Up to this point, we have not specified the orientation of \tilde{J}^2 , which can now be fixed as counterclockwise. Let γ_i be a single small loop around 0, 1, ∞ , and $y_{1,2}$, for $i = 1, \dots, 5$, respectively. We take lifts $\hat{\gamma}_i$ of γ_i by ζ and notice that the end points of $\hat{\gamma}_i$ differ by J^{k_i} , $0 \leq k_i \leq n-1 = 2k+1$, $1 \leq i \leq 5$.

Now take D as the open unitary complex disk at the origin. Since ζ is the quotient map $(./J) : \overline{M} \rightarrow \overline{M}/J$, there is a coordinate chart $z : D \rightarrow \overline{M}$ with $z(0) = p_1$ such that $\zeta(z) = z^n$. By taking γ_1 small enough to be in $\zeta(z(D))$, we conclude that $k_1 = 1$. The same reasoning will give $k_{2,3} = -1$. If we had taken $z(0) = r_1$, then $\zeta(z) = y_1 + z^{n/2}$ and so $k_4 = 2$. By the same reasoning $k_5 = -2$. Let us define $\mathcal{A} := \mathbb{C} \setminus \{0, 1, s, y_1, y_2\}$.

The numbers k_i naturally determine a homomorphism $H : \pi_1(\mathcal{A}) \rightarrow \mathbb{Z}_n \oplus \mathbb{Z}_{n/2}$, of which the kernel is $\zeta_*(\pi_1(\overline{M} \setminus \{p_{1,2}, q_{1,2}, r_{1,\dots,4}\})) \subset \pi_1(\mathcal{A})$. Let us now define the following compact Riemann surface:

$$\overline{R} := \left\{ (v, w) \in \hat{\mathbb{C}} \times \hat{\mathbb{C}} : w^{2(k+1)} = \frac{v-s}{v(v-1)} \cdot \left(\frac{v-y_1}{v-y_2} \right)^2 \right\}. \quad (8)$$

From (8) one easily sees that $(v, w) \rightarrow (v, e^{2\pi i/n} w)$ is a biholomorphism of \overline{R} , exactly with the following fixed points: $(0, \infty)$, $(1, \infty)$, $(\infty, 0)$, $(s, 0)$, each of order n , and $(y_1, 0)$, (y_2, ∞) , each of order $n/2$. The Riemann-Hurwitz formula gives

$$\frac{1}{2}[4 \cdot 1 \cdot (n-1) + 2 \cdot 2 \cdot (n/2 - 1)] - n + 1 = 4k + 1,$$

namely the same genus as \overline{M} . Moreover, the projection map $v : \overline{R} \rightarrow \hat{\mathbb{C}}$, namely $(v, w) \rightarrow v$, is such that $v_*(\pi_1(\overline{R} \setminus w^{-1}(\{0, \infty\})))$ also represents the kernel of H . From [18, p159] we conclude that \overline{M} is biholomorphic to \overline{R} .

Now we use (6-8) in order to read off the Weierstrass data

$$g = a_0 v w^k \quad \text{and} \quad dh = \frac{b_0(v-y_2)w^{k+1}dv}{(v-s)(v-y_1)}, \quad (9)$$

where $a_0 \in \mathbb{R}_+^*$ and $b_0 \in ((\mathbb{R}_+ \times i\mathbb{R}) \setminus (\{0\} \times i\mathbb{R}_-)) \subset \mathbb{C}$. These sets containing a_0 and b_0 were established that way because \tilde{M} can be suitably rotated and, if necessary, replaced by its antipodal image.

4. The symmetries of the minimal immersions

From (iv) and the rigidity of \tilde{M} we have $|\Delta| \geq 2(\varrho + 3) = 4n$. Since $|\mathcal{G}| = n$ and $|\Delta : \mathcal{G}| \leq 4$, equality follows. Any $A \in \Delta$ either fixes the ends $p_{1,2}$ or interchanges them. In any case A^2 fixes the ends, and so $A^2 \in \mathcal{G}$. This means that $\Delta/\mathcal{G} = \{f_0, f_1, f_2, f_3\}$ is a group isomorphic to $\mathbb{Z}_2 \oplus \mathbb{Z}_2$, and each f_i is an automorphism in $\overline{M}/J \cong \hat{\mathbb{C}}$. Up to re-indexing we assume that

- f_0 and f_1 are holomorphic involutions;
- f_2 and f_3 are anti-holomorphic involutions with $f_3 = f_1 \circ f_2$;

- f_0 and f_2 fix the points $0, 1, s$ and ∞ .
- f_1 and f_3 interchange $0 \leftrightarrow \infty$ and $1 \leftrightarrow s$.

It is immediate that $f_0 = id_{\hat{\mathbb{C}}}$ and $s \in \mathbb{R} \setminus \{0, 1\}$, because f_2 keeps invariant exactly *one* circumference of $\hat{\mathbb{C}}$, namely $\hat{\mathbb{R}}$. Therefore

$$f_0(v) = v, \quad f_1(v) = \frac{s}{v}, \quad f_2(v) = \bar{v} \quad \text{and} \quad f_3(v) = \frac{\bar{s}}{\bar{v}}.$$

We now get more information about $y_{1,2}$. From (iv) we have $|Iso(\tilde{M}/\mathcal{T})| \geq 4n$, $n = \text{ord}(J)$. This implies the existence of automorphisms of \overline{M} that interchange the points $p_1 \leftrightarrow p_2$ and $q_1 \leftrightarrow q_2$. Recall that a symmetry which fixes one of the points p_i, q_i must also fix the others. Hence there exists three distinct automorphisms of \overline{M} , $\sigma_{0,1,2}$, such that any $A \in \Delta$ belongs to one of the sets in the following table:

automorphisms	fix p_i	interch. p_i
holom.	\mathcal{G}	$\sigma_0 \mathcal{G}$
anti-holom.	$\sigma_1 \mathcal{G}$	$\sigma_2 \mathcal{G}$

Let us call $\frac{1}{2}\mathcal{T}_\theta$ the translation in \mathbb{R}^3 by $(0, 0, 1)$, followed by a counterclockwise rotation of angle θ around Ox_3 . A little reflection about all isometries of \mathbb{R}^3/\mathcal{T} which either fix or interchange $q_{1,2}$ will establish that:

- σ_0 corresponds to a 180° -rotation around a line $\ell_0 \perp Ox_3$ at $x_3 = 1/2$;
- σ_1 can be taken as a 180° -rotation around a line $\ell_1 \perp Ox_3$ at $x_3 = 0$;
- σ_2 corresponds to a screw motion $\frac{1}{2}\mathcal{T}_\theta$ for a certain θ .

Notice that $\frac{1}{2}\mathcal{T}_\theta$ is orientation-reversing, thus anti-holomorphic. Moreover, \tilde{M} can be re-positioned in \mathbb{R}^3 in such a way that $\sigma_1(a, b, c) = (a, -b, -c)$. Hence $J \circ \sigma_1(a, b, c) = ((a - ib)e^{2\pi i/n}, c)$, namely a reflection in the plane $x_2/x_1 = \tan(\pi/n)$. This means that we have included reflection in a vertical plane containing Ox_3 . We have not considered σ_2 as a reflection in the plane $x_3 = 1/2$, for this will happen if and only if ℓ_0 belongs to a vertical plane of reflectional symmetry.

Now consider the points \tilde{r}_i of \mathcal{S} such that $\tilde{r}_i/\mathcal{T} = r_i$. Therefore, σ_0 interchanges $r_1 \leftrightarrow r_2$ and $r_3 \leftrightarrow r_4$, while σ_1 interchanges $r_1 \leftrightarrow r_3$ and $r_2 \leftrightarrow r_4$. From σ_1 we have $y_{1,2} \in \mathbb{R}$ and from σ_0 it follows that $y_1 \cdot y_2 = s$.

Notice that (8) implies

$$v(v-1)(v-s) = \frac{(v-s)^2(v-y_1)^2}{w^{2(k+1)}(v-y_2)^2},$$

and so $v(v-1)(v-s)$ has a well-defined square root on \overline{R} . One rewrites (9) as

$$g = a_0 v w^k \quad \text{and} \quad dh = \frac{b_0 dv}{\sqrt{v(v-1)(v-s)}}. \quad (10)$$

Now we are going to read off some information about the constant b_0 at (10). Recall that \tilde{p}_1 corresponds to $x_3 = 1$ and \tilde{p}_2 to $x_3 = 0$. Therefore, any path on \tilde{M} starting at \tilde{q}_i

and diverging to the end \tilde{p}_1 will be taken by ζ to a curve in $\hat{\mathbb{C}}$ connecting 0 and $\zeta(q_i)$. This latter is homotopically the (oriented) segment $[0, \zeta(q_i))$, for any extra loop with base point at 0 or $\zeta(q_i)$ gives $Re \int dh = 0$. Our analysis can be now separated in three different cases:

Case I: $s < 0$. Suppose $(0, 0, 1) = \tilde{q}_1$. By taking $v(t) = t$, $0 < t < 1$, then $Re \int dh = 0 \Leftrightarrow b_0 \in \mathbb{R}_+^*$. On the other hand, if $(0, 0, 1) = \tilde{q}_2$ and $s < t < 0$, then $Re \int dh = 0 \Leftrightarrow b_0 \in i\mathbb{R}_+^*$.

Case II: $0 < s < 1$. Suppose $(0, 0, 1) = \tilde{q}_1$. In this case, for $\eta := dt/\sqrt{|t(t-1)(t-s)|}$ one must have

$$1 = Re(b_0) \int_0^s \eta = |Im(b_0)| \int_s^1 \eta. \quad (11)$$

Therefore, b_0 can be neither real nor pure imaginary. Since $[0, 1]$ is homotopically $\hat{\mathbb{R}} \setminus (0, 1)$, then $1 = Re(b_0) \int_1^\infty \eta = |Im(b_0)| \int_{-\infty}^0 \eta$, which is equivalent to (11). Indeed, the change $t \rightarrow s/t$ shows that $\int_0^s \eta = \int_1^\infty \eta$, while the changes $t \rightarrow 1 - 1/t$ for $\int_{-\infty}^0 \eta$ and $t \rightarrow 1 + (s-1)t$ for $\int_s^1 \eta$ show equality between these last two integrals. On the other hand, if $(0, 0, 1) = \tilde{q}_2$ and $0 < t < s$, then $Re \int dh = 0 \Leftrightarrow b_0 \in i\mathbb{R}_+^*$.

Case III: $s \geq 1$. Suppose $(0, 0, 1) = \tilde{q}_1$. By taking $v(t) = t$, $0 < t < 1$, then $Re \int dh = 0 \Leftrightarrow b_0 \in i\mathbb{R}_+^*$. On the other hand, if $(0, 0, 1) = \tilde{q}_2$ and $0 < t < s$, one must have

$$1 = Re(b_0) \int_0^1 \eta = |Im(b_0)| \int_1^s \eta. \quad (12)$$

Therefore, b_0 can be neither real nor pure imaginary. Since $[0, s]$ is homotopically $\hat{\mathbb{R}} \setminus (0, s)$, then $1 = Re(b_0) \int_s^\infty \eta = |Im(b_0)| \int_{-\infty}^0 \eta$, which is equivalent to (12) by suitable changes of variable.

We see that Cases I-III are independent of the real numbers $y_{1,2}$. For any interval $(a, b) \subset \mathbb{R}^*$, since $y_1 \cdot y_2 = s$, then $y_1 \in (a, b) \Leftrightarrow y_2 \in (s/a, s/b)$ for $s < 0$, $y_2 \in (s/b, s/a)$ for $s > 0$. These are all the possibilities:

- i) $y_{1,2} < s < 0 < y_{2,1} < 1$,
- ii) $s < y_{1,2} < 0 < 1 < y_{2,1}$,
- iii) $y_{1,2} < y_{2,1} < 0 < s < 1$,
- iv) $0 < y_{1,2} < s < 1 < y_{2,1}$,
- v) $0 < s < y_{1,2} < y_{2,1} < 1$,
- vi) $y_{1,2} < y_{2,1} < 0 < 1 < s$,
- vii) $0 < y_{1,2} < 1 < s < y_{2,1}$,
- viii) $0 < 1 < y_{1,2} < y_{2,1} < s$.

At this point we have just listed the considerable amount of 32 possibilities. Nevertheless, this number will quickly drop to only four items until next section. From (8) and (10) we have

$$g^{2(k+1)} = a_0^{2(k+1)} v^{k+2} \left(\frac{v-s}{v-1} \right)^k \left(\frac{v-y_1}{v-y_2} \right)^{2k}. \quad (13)$$

For Case I.i, $(0, 0, 1) = \tilde{q}_1$ implies $b_0 > 0$. After a suitable rotation of \tilde{M} around Ox_3 , either $v \in (y_1, s)$ or $v \in (y_2, 1)$ will give $g \in \mathbb{R}_+^*$. Hence ϕ_2 is real and never zero on these stretches, and so $Re \int \phi_2 \neq 0$. But $\zeta^{-1}(\{1, s, y_{1,2}\}) \subset Ox_3$, a contradiction. Therefore I.i implies $(0, 0, 1) = \tilde{q}_2$. For Case I.ii, $(0, 0, 1) = \tilde{q}_2$ implies $ib_0 < 0$. After a suitable rotation, either $v \in (s, y_1)$ or $v \in (1, y_2)$ will give $g \in \mathbb{R}_+^*$, and the same reasoning leads to the contradiction $Re \int \phi_2 \neq 0$. Hence I.ii implies $(0, 0, 1) = \tilde{q}_1$.

For any of the Cases II.iii, II.iv or II.v, if $(0, 0, 1) = \tilde{q}_1$ then $Re \int dh \neq 0$ for some stretch $v \in (a, b)$, $a, b \in \{s, 1, y_{1,2}\}$. Once again, this contradicts $\zeta^{-1}(\{1, s, y_{1,2}\}) \subset Ox_3$ and therefore $(0, 0, 1) = \tilde{q}_2$. The same reasoning shows that III.vi, III.vii and III.viii imply $(0, 0, 1) = \tilde{q}_1$.

At this point, since either $y_1 < y_2$ or $y_2 < y_1$, we have just reduced our analysis to 16 Cases. Before going ahead, notice that both II.iv and III.vii fail. This is because \tilde{M} can be suitably rotated about Ox_3 to get g real for $\max\{y_1, y_2\} \leq v < \infty$, while dh is pure imaginary on this stretch. Therefore, $dh \cdot dg/g$ is pure imaginary there, implying that \tilde{M}/\mathcal{T} has horizontal straight lines connecting its ends to points r_i , $1 \leq i \leq 4$. Since these points are in Ox_3 , some of them should coincide with either q_1 or q_2 , contradicting the embeddedness of \tilde{M} . Now they remain the other 12 cases.

5. Reduction of cases by geometric arguments

We have just concluded that $(0, 0, 1) = \tilde{q}_2$ exactly for I.i, II.iii and II.v, all with $b_0 \in i\mathbb{R}_+^*$, while $(0, 0, 1) = \tilde{q}_1$ exactly for I.ii, III.vi and III.viii, the latter two also with $b_0 \in i\mathbb{R}_+^*$, while $b_0 \in \mathbb{R}_+^*$ for the former.

Now consider i, ii, v and viii. If y_1 comes immediately after s or vice-versa, then (13) shows that real values of v between s and y_1 will make g vary along some meridians of $\tilde{\mathbb{C}}$, from 0 to 0, but never reaching ∞ . Therefore, dg/g will be real, while dh is real and never zero. Hence these stretches are plane geodesics of \tilde{M} . However, since they connect \tilde{q}_2 with \tilde{r}_1 or \tilde{r}_3 , which lie in Ox_3 , then any of these curves will cross the vertical axis at a third point in between, where the normal vector will not be vertical. But this contradicts the embeddedness of \tilde{M} , since \tilde{J}^2 is a $2\pi/(k+1)$ -rotation around Ox_3 . Therefore, cases i, ii, v and viii are reduced to

- i) $y_2 < s < 0 < y_1 < 1$,
- ii) $s < y_2 < 0 < 1 < y_1$,
- v) $0 < s < y_2 < y_1 < 1$,
- viii) $0 < 1 < y_1 < y_2 < s$.

In Section 3, we concluded that \tilde{J} is a rotation around Ox_3 followed by reflection in Ox_1x_2 . Therefore, up to re-indexing, we assume that $r_{1,2}$ lie between $x_3 = 0$ and $x_3 = 1$. If r_1 is above r_2 , this will force $y_2 < y_1$ at iii and vi due to $Re \int dh$, namely the third coordinate of \tilde{M} . But $y_2 < y_1$ drops case iii, for (13) shows that this would give two geodesics in the plane $\Pi : x_2/x_1 = -\tan \frac{k\pi}{2(k+1)}$, the one bounded and connecting q_1 with q_2 , the other unbounded and connecting the end p_2 with r_2 . Moreover, by (13) one sees that both should be in the same half-plane determined by $Ox_3 \subset \Pi$ and therefore would cross, contradicting the embeddedness of \tilde{M} .

The assumption of r_1 above r_2 also drops case ii because of the following argument: after a suitable rotation of \tilde{M} around Ox_3 , $v \in (y_2, 0)$ will give $g \in \mathbb{R}_+^*$. Hence, the corresponding geodesic in \tilde{M} will have to cross the vertical axis at a point where the normal vector will not be vertical. But this contradicts the embeddedness of \tilde{M} , since \tilde{J}^2 is a $2\pi/(k+1)$ -rotation about Ox_3 . This means, r_1 above r_2 cancels cases ii and iii. By very similar arguments, assuming r_2 above r_1 , cases ii and iii fail again. Now we remain with

- i) $y_2 < s < 0 < y_1 < 1$,
- v) $0 < s < y_2 < y_1 < 1$,
- vi) $y_2 < y_1 < 0 < 1 < s$,
- viii) $0 < 1 < y_1 < y_2 < s$.

Notice from statement vi that r_1 is above r_2 if and only if $y_2 < y_1$. It is totally equivalent to study this one or its reverse, and hence our reduction is complete. The next sections are devoted to the study of the remaining cases.

6. Non-solvability of the period problems for i, v and vi

We begin with case i. In Section 3 one saw that \overline{M} is biholomorphic to \overline{R} given by (8). Now we closely follow the arguments from [16, p453]. By labelling $a = 1/\sqrt{|s|}$, $b = |y_1/y_2|^{\frac{1}{2}}$, $B = \sqrt[k+1]{b}$ and making the changes $z = av$, $u = B/w$, an easy computation shows that \overline{R} is biholomorphic to

$$\overline{N} := \left\{ (z, u) \in \hat{\mathbb{C}} \times \hat{\mathbb{C}} : u^{2(k+1)} = \frac{z(z-a)}{az+1} \cdot \left(\frac{bz+1}{z-b} \right)^2 \right\}.$$

Notice that we still have $J(z, u) = (z, e^{i\pi/(k+1)}u)$. Define $A := a_0 B^k/a$, so with u and z the Weierstrass data become

$$g = Azu^{-k} \quad \text{and} \quad dh = \frac{ab_0 dz}{\sqrt{z(z-a)(az+1)}}.$$

In Section 4 we saw that \overline{M} is endowed with an automorphism σ_2 , which in \tilde{M} corresponds to a screw motion $\frac{1}{2}\mathcal{T}_\theta$, for a certain θ . From the Weierstrass data, it is easy to see that $\theta = 0$ and so σ_2 represents half of the vertical translation \mathcal{T} . Now recall that $b_0 \in i\mathbb{R}_+^*$. From arguments very similar to [16, p461], one concludes that

$$\sigma_2(z, u) = (-1/\bar{z}, 1/\bar{u})$$

and

$$\sigma_2(gdh) = -A^2 \overline{dh/g}, \quad \sigma_2(dh/g) = -\overline{gdh}/A^2 \quad \text{and} \quad \sigma_2(dh) = \overline{dh}. \quad (14)$$

As σ_2 corresponds to a rigid motion in \mathbb{R}^3 , then $A^2 = 1$. Hence $A = 1$ because A is positive. Defining $N := \overline{N} \setminus z^{-1}(\{0, \infty\})$, the immersion $X : N \rightarrow \mathbb{R}^3/\mathcal{T}$ will be period free if and only if

$$\int_\gamma dh/g = \int_\gamma \overline{gdh}, \quad \operatorname{Re} \int_\gamma dh \in 2\mathbb{Z}, \quad \forall [\gamma] \in H_1(N). \quad (15)$$

Now observe that $b = ay_1$, with $0 < y_1 < 1$, and consider the curve c represented in Figure 3. For $\tilde{g} := e^{-i\pi/(2k+2)}g$, a suitable choice of logarithmic branch shows that the Weierstrass data (\tilde{g}, dh) take the intervals $a < z < b$ and $-1/b < z < -1/a$ to geodesics in planes parallel to $x_1 = 0$. Let c^+ denote the stretch of c in the upper half plane. If X is period free, then

$$\operatorname{Re} \int_{c^+} \tilde{g}dh = \operatorname{Re} \int_{c^+} dh/\tilde{g},$$

or equivalently

$$-\operatorname{Re} \int_{-1/b < z < b} \tilde{g}dh = \operatorname{Re} \int_{a < z < \infty} dh/\tilde{g}. \quad (16)$$

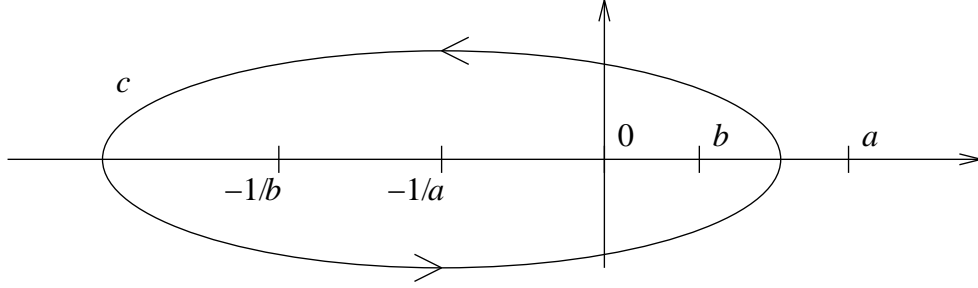


Figure 3: The curve c in the complex plane.

From (14) we see that

$$\operatorname{Re} \int_{a < z < \infty} dh/\tilde{g} = \operatorname{Re} \int_{a < z < \infty} \sigma_2(\tilde{g}dh) = -\operatorname{Re} \int_{-1/a < z < 0} \tilde{g}dh.$$

Now (16) becomes

$$\operatorname{Re} \int_{-1/b < z < -1/a} \tilde{g}dh + \operatorname{Re} \int_{0 < z < b} \tilde{g}dh = 0. \quad (17)$$

By keeping the same logarithmic branch, on $-1/b < z < -1/a$ we see that dh is positive and $\tilde{g} \in e^{i\pi(k-1)/(2k+2)}\mathbb{R}_+$, while on $0 < z < b$ on has dh negative and $\tilde{g} \in e^{i\pi(k-1)/(2k+2)}\mathbb{R}_-$. Hence (17) is equivalent to

$$\cos\left(\frac{\pi}{2} \cdot \frac{k-1}{k+1}\right) \cdot \left[\int_{-1/b}^{-1/a} |g|dh + \int_0^b |g|dh \right] = 0, \quad (18)$$

which never holds.

A three-dimensional sketch of $X(N)$ is presented in Figure 4. It is important to note that the arguments presented herein differ from the ones in [16, pp460-2] and [2, pp176-180]. Of course, the surfaces are not the same, but the arguments are adaptable. For instance, one could rewrite (18) in [16, p462] by suppressing the first integral and taking $b = a$ in the second.

For reasons that will soon be clear, we shall invert order and study case vi before v. Take a, b, B, z and u as before. Hence \bar{R} is biholomorphic to

$$\bar{N} := \left\{ (z, u) \in \hat{\mathbb{C}} \times \hat{\mathbb{C}} : u^{2(k+1)} = \frac{z(z-a)}{az-1} \cdot \left(\frac{bz+1}{z+b} \right)^2 \right\},$$

and we still have $J(z, u) = (z, e^{i\pi/(k+1)}u)$. Take A as before, so with u and z the Weierstrass data become

$$g = Azu^{-k} \quad \text{and} \quad dh = \frac{ab_0 dz}{\sqrt{z(z-a)(az-1)}}. \quad (19)$$

From Section 4, the automorphism σ_2 corresponds to a screw motion $\frac{1}{2}\mathcal{T}_\theta$, now with $\theta = -\pi/(k+1)$. Again $b_0 \in i\mathbb{R}_+^*$, hence

$$\sigma_2(z, u) = (1/\bar{z}, e^{-i\pi/(k+1)}/\bar{u})$$

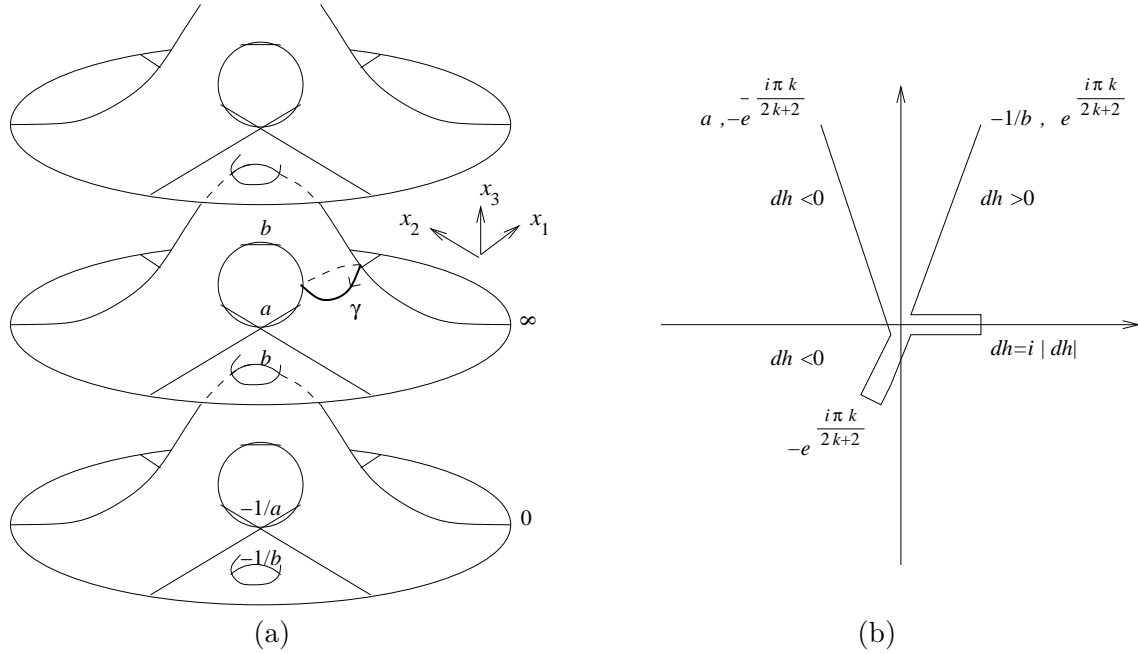


Figure 4: (a) The surface $X(N)$ for $k = 1$; (b) The Gauß map on symmetry curves.

and

$$\sigma_2(gdh) = e^{-\frac{i\pi}{k+1}} A^2 \overline{dh/g}, \quad \sigma_2(dh/g) = e^{\frac{i\pi}{k+1}} \overline{gdh}/A^2 \quad \text{and} \quad \sigma_2(dh) = \overline{dh}. \quad (20)$$

As σ_2 corresponds to a rigid motion in \mathbb{R}^3 , then $A = 1$. Defining $\mathcal{N} := \overline{\mathcal{N}} \setminus z^{-1}(\{0, \infty\})$, the immersion $X : \mathcal{N} \rightarrow \mathbb{R}^3/\mathcal{T}$ will be period free if and only if

$$\int_{\gamma} dh/g = \int_{\gamma} \overline{gdh}, \quad \text{Re} \int_{\gamma} dh \in 2\mathbb{Z}, \quad \forall [\gamma] \in H_1(\mathcal{N}).$$

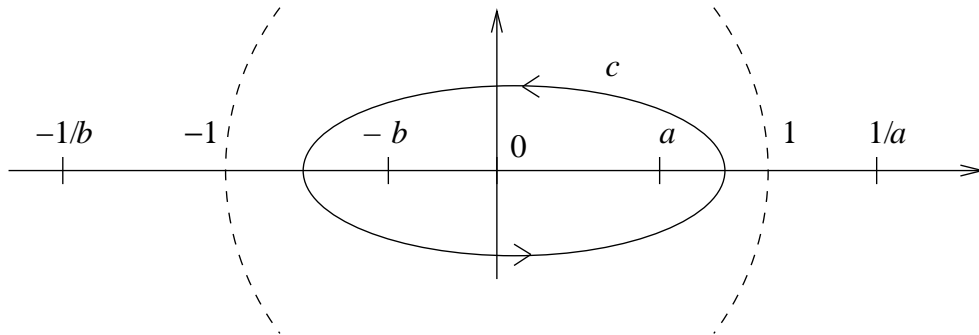


Figure 5: The curve c in the complex plane.

Now observe that a and b are both in $(0, 1)$, and consider the curve c represented in Figure 5. Take \tilde{g} as before. A suitable choice of logarithmic branch shows that the Weierstrass data (\tilde{g}, dh) take the intervals $a < z < 1/a$ and $0 < z < \infty$ to geodesics in planes parallel to $x_1 = 0$. Let c^+ denote the stretch of c in the upper half plane. If X is period free, then

$$\text{Re} \int_{c^+} \tilde{g} dh = \text{Re} \int_{c^+} dh/\tilde{g},$$

or equivalently

$$- \operatorname{Re} \int_{-b < z < a} \tilde{g} dh = \operatorname{Re} \int_{1/a < z < -1/b} dh / \tilde{g}, \quad (21)$$

with z passing through infinity. The right-hand side of (21) equals

$$\operatorname{Re} \int_{1/a < z < -1/b} \overline{dh/\tilde{g}} \stackrel{(20)}{=} \operatorname{Re} \int_{1/a < z < -1/b} e^{\frac{i\pi}{k+1}} \sigma_2(\tilde{g} dh) = \operatorname{Re} \int_{-b < z < a} e^{\frac{i\pi}{k+1}} \tilde{g} dh.$$

Hence (21) holds if and only if $2 \cos(\frac{\pi}{2k+2}) \cdot \operatorname{Re} \int_{-b}^a g dh = 0$. But since $g dh$ is pure imaginary for $0 < z < a$, (21) is equivalent to $\operatorname{Re} \int_{-b}^0 g dh = 0$. This never holds, for

$$\operatorname{Re} \int_{-b}^0 g dh = -\operatorname{Re} \int_{-b}^0 e^{\frac{i\pi}{2k+2}} |g dh| = -\cos\left(\frac{\pi}{2k+2}\right) \cdot \int_{-b}^0 |g dh| < 0.$$

A three-dimensional sketch of $X(\mathcal{N})$ is depicted in Figure 6. As remarked at the introduction, one easily identifies the presence a Gaussian geodesic in cases i and vi. One period is essentially due to $\int |g dh|$ along it, and consequently never vanishes. That is why we surveyed cases i and vi together. In case v there is no Gaussian geodesic, but Horgan saddle. The reader will notice that one period never vanishes again, namely around that saddle. In spite of their oddness, Horgan saddles were recently found in singly periodic examples (see [30]).

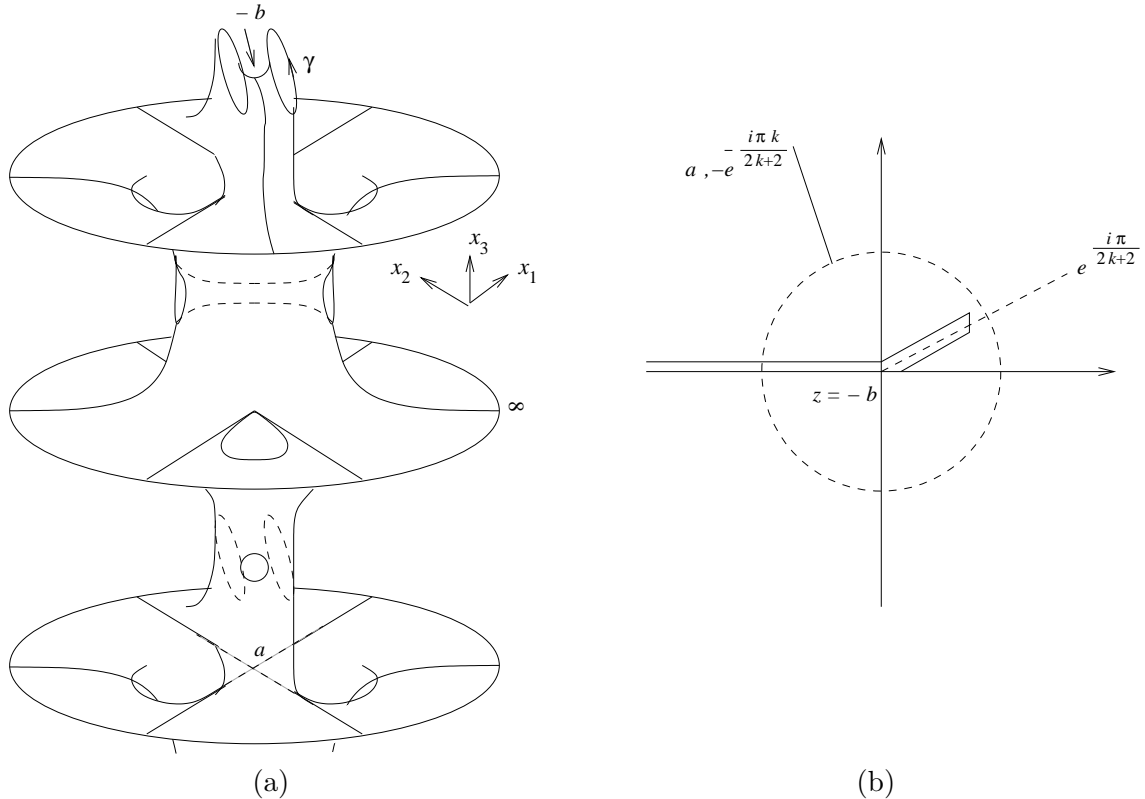


Figure 6: (a) The surface $X(\mathcal{N})$ for $k = 1$; (b) The Gauß map on symmetry curves.

We conclude this section with case v. By taking all parameters as before, one sees that

\overline{R} is biholomorphic to

$$\overline{N} := \left\{ (z, u) \in \hat{\mathbb{C}} \times \hat{\mathbb{C}} : u^{2(k+1)} = \frac{z(z-a)}{az-1} \cdot \left(\frac{bz-1}{z-b} \right)^2 \right\},$$

again with $J(z, u) = (z, e^{i\pi/(k+1)}u)$. The Weierstrass data coincide with (19), but now $a \in (1, \infty)$ and $b \in (1, a)$. The automorphism σ_2 is once more the screw motion $\frac{1}{2}\mathcal{T}_\theta$ with $\theta = \pi/(k+1)$ and (20) still holds, with $A = 1$. Defining $N := \overline{N} \setminus z^{-1}(\{0, \infty\})$, the immersion $X : N \rightarrow \mathbb{R}^3/\mathcal{T}$ will be period free if and only if

$$\int_\gamma dh/g = \int_\gamma \overline{g}d\overline{h}, \quad \operatorname{Re} \int_\gamma dh \in 2\mathbb{Z}, \quad \forall [\gamma] \in H_1(N).$$

Now consider the curve c represented in Figure 7. By using \tilde{g} and a suitable choice of logarithmic branch, the pair (\tilde{g}, dh) takes the intervals $b < z < a$ and $1/a < z < 1/b$ to geodesics in planes parallel to $x_1 = 0$.

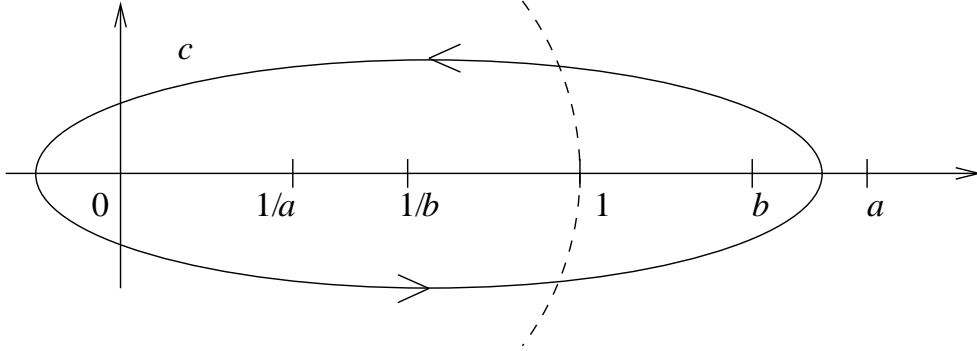


Figure 7: The curve c in the complex plane.

Let c^+ denote the stretch of c in the upper half plane. If X is period free, then

$$\operatorname{Re} \int_{c^+} \tilde{g}dh = \operatorname{Re} \int_{c^+} dh/\tilde{g},$$

or equivalently

$$-\operatorname{Re} \int_{0 < z < b} \tilde{g}dh = \operatorname{Re} \int_{a < z < \infty} dh/\tilde{g}. \quad (22)$$

From (20) we see that

$$\operatorname{Re} \int_{a < z < \infty} dh/\tilde{g} = \operatorname{Re} \int_{a < z < \infty} e^{\frac{i\pi}{k+1}} \sigma_2(\tilde{g}dh) = \operatorname{Re} \int_{0 < z < 1/a} e^{\frac{i\pi}{k+1}} \tilde{g}dh,$$

whereas

$$\operatorname{Re} \int_{0 < z < b} \tilde{g}dh = \operatorname{Re} \int_{0 < z < 1/a} \tilde{g}dh + \operatorname{Re} \int_{1/b < z < b} \tilde{g}dh, \quad (23)$$

because \tilde{g} and dh are real and pure imaginary for $1/a < z < 1/b$, respectively. For $0 < z < 1/a$, $g = -|g|$ and $dh = i|dh|$, and so the last integral from (23) cancels with the right-hand side of (22). This leads to $\operatorname{Re} \int_{0 < z < 1/a} \tilde{g}dh = 0$, which never holds. See Figure 8 for a sketch of $X(N)$.

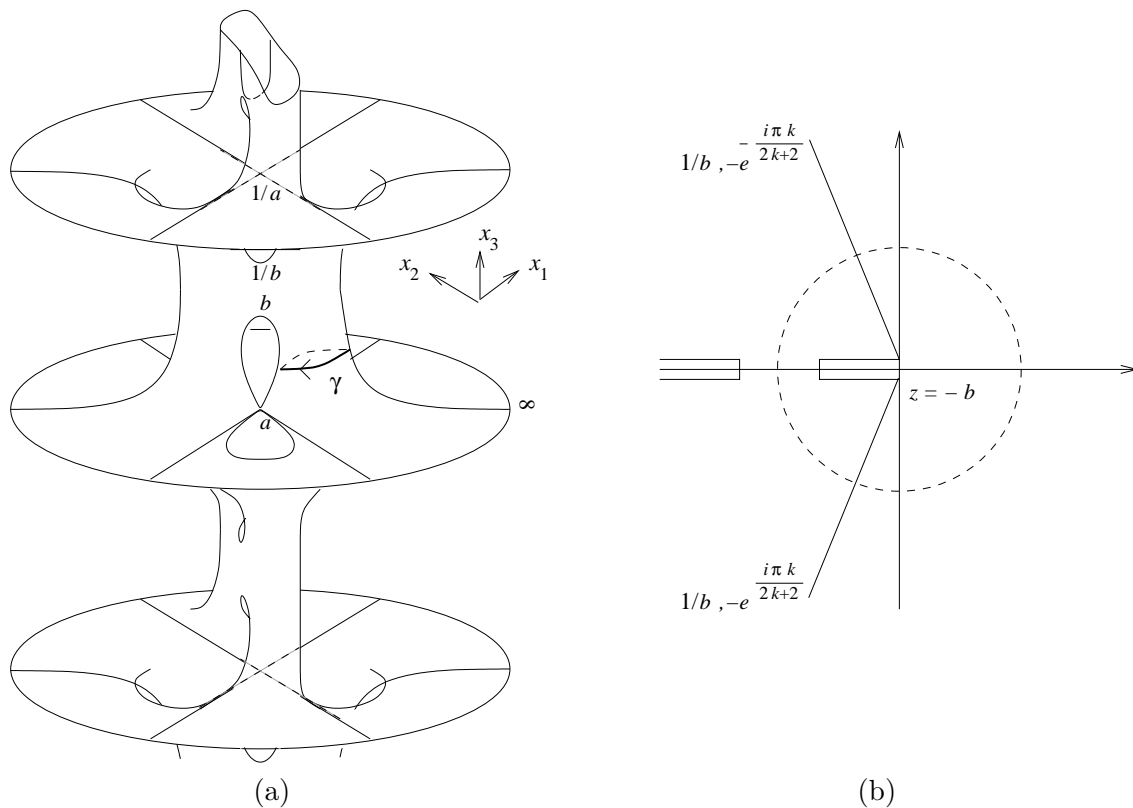


Figure 8: (a) The surface $X(\mathbf{N})$ for $k = 1$; (b) The Gauß map on symmetry curves.

7. The Hoffman-Wohlgemuth surfaces

We recall that $0 < 1 < y_1 < y_2 < s$ for case viii, thus with all parameters positive as in case v. Therefore \bar{R} is again biholomorphic to \bar{N} , but now with $a \in (0, 1)$ and $b \in (a, 1)$. Both (19) and (20) still hold, hence $A = 1$.

Now consider the curves γ , Γ , δ and Δ represented in Figure 9. Up to homotopy, the curve $\delta + \Delta = \Gamma - \gamma$ is invariant under the map $z \rightarrow 1/z$.

Recalling that $\tilde{g} = e^{-i\pi/(2k+2)}g$ and defining $\hat{g} := e^{-i\pi k/(2k+2)}g$, the immersion $X : \mathbf{N} \rightarrow \mathbb{R}^3/\mathcal{T}$ will be period free if and only if

$$\operatorname{Re} \int_{\gamma} \tilde{g} dh = \operatorname{Re} \int_{\gamma} dh/\tilde{g} \quad (24)$$

and

$$\operatorname{Re} \int_{\delta} \hat{g} dh = \operatorname{Re} \int_{\delta} dh/\hat{g}. \quad (25)$$

Let us take $\psi := \sigma_0 \circ \sigma_1 \circ \sigma$, hence $\psi(z, u) = (1/\bar{z}, 1/\bar{u})$, $\psi(g) = 1/\bar{g}$ and $\psi(dh) = -\overline{dh}$. Consequently,

$$\int_{\delta+\Delta} g dh = - \int_{\psi(\delta+\Delta)} g dh = - \int_{\delta+\Delta} \psi(g dh) = \int_{\delta+\Delta} \overline{dh/g}. \quad (26)$$

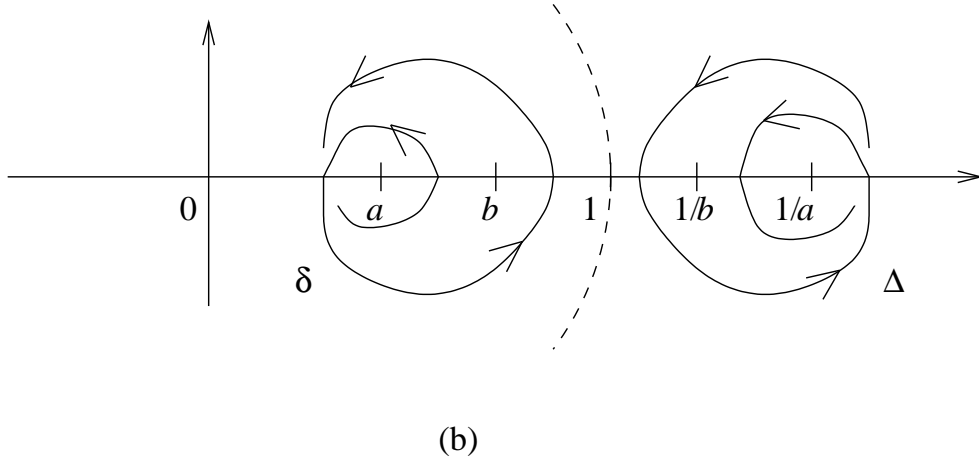
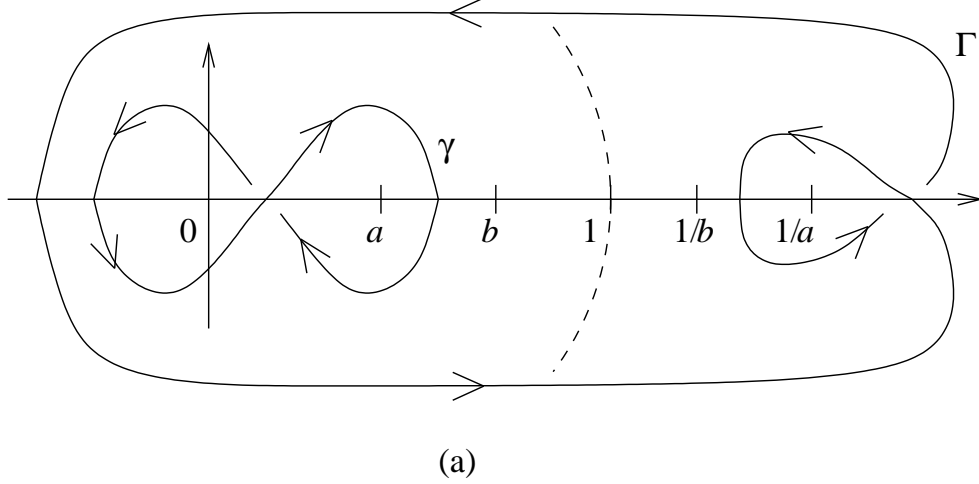


Figure 9: (a) The curves γ , Γ and (b) δ , Δ in the complex plane.

Moreover, $\operatorname{Re} \int_{\gamma} dh/\tilde{g} = \operatorname{Re} \int_{\Gamma} \overline{dh/\tilde{g}} - \operatorname{Re} \int_{\delta+\Delta} \overline{dh/\tilde{g}} \stackrel{(26)}{=} -\operatorname{Re} \int_{\Gamma} \psi(\tilde{g}dh) - \operatorname{Re} \int_{\delta+\Delta} \tilde{g}dh$, namely

$$\operatorname{Re} \int_{\gamma} dh/\tilde{g} = -\operatorname{Re} \int_{\gamma} \tilde{g}dh - \operatorname{Re} \int_{\delta+\Delta} \tilde{g}dh. \quad (27)$$

With (27) one rewrites (24) as

$$2\operatorname{Re} \int_{\gamma} \tilde{g}dh = -\operatorname{Re} \int_{\delta+\Delta} \tilde{g}dh. \quad (28)$$

Up to a homothety in \mathbb{R}^3 , appropriate choices of the logarithmic branch will give

$$\tilde{g}(t) = e^{-\frac{i\pi}{2k+2} t^{\frac{k+2}{2k+2}}} \cdot \left(\frac{1-at}{a-t}\right)^{\frac{k}{2k+2}} \cdot \left(\frac{b-t}{1-bt}\right)^{\frac{k}{k+1}}, \quad dh(t) = \frac{idt}{\sqrt{t(a-t)(1-at)}}, \quad 0 < t < a,$$

$$\tilde{g}(t) = e^{\frac{i\pi(k-1)}{2k+2} t^{\frac{k+2}{2k+2}}} \cdot \left(\frac{1-at}{t-a}\right)^{\frac{k}{2k+2}} \cdot \left(\frac{b-t}{1-bt}\right)^{\frac{k}{k+1}}, \quad dh(t) = \frac{dt}{\sqrt{t(t-a)(1-at)}}, \quad t^{\pm 1} \in (a, b),$$

and

$$\hat{g}(t) = t^{\frac{k+2}{2k+2}} \cdot \left(\frac{1-at}{t-a} \right)^{\frac{k}{2k+2}} \cdot \left(\frac{b-t}{1-bt} \right)^{\frac{k}{k+1}}, dh(t) = \frac{dt}{\sqrt{t(t-a)(1-at)}}, \quad a < t < b.$$

It is easy to check that $z \rightarrow 1/\bar{z}$ is now an isometry for the minimal surface, which implies $\int gdh = 0$ on $b < z < 1/b$. Therefore (25) and (28) are explicitly given by

$$I_0 := \int_a^b \frac{t^{1/(2k+2)} [(b-t)/(1-bt)]^{k/(k+1)} dt}{[(1-at)(t-a)^{2k+1}]^{1/(2k+2)}} = \int_a^b \frac{[(1-bt)/(b-t)]^{k/(k+1)} dt/t}{[t(t-a)(1-at)^{2k+1}]^{1/(2k+2)}} =: I_1 \quad (29)$$

and

$$J_0 := \int_0^a \frac{t^{1/(2k+2)} [(b-t)/(1-bt)]^{k/(k+1)} dt}{[(1-at)(a-t)^{2k+1}]^{1/(2k+2)}} = \cos\left(\frac{\pi}{2k+2}\right) \cdot J_1, \quad (30)$$

where $J_1 := J_+ + J_-$ with

$$J_{\pm} := \int_{(a,b)_{\pm 1}} \frac{t^{1/(2k+2)} [(b-t)/(1-bt)]^{k/(k+1)} dt}{[(1-at)(t-a)^{2k+1}]^{1/(2k+2)}}. \quad (31)$$

Notice that $I_0 = J_+$ and $I_1 = J_-$. Except for I_1 and J_- , it is easy to see that all integrals in (29-31) are continuous at $b = 1$. For I_1 and J_- make the changes $t = b - u^{k+1}$ and $t = (1+u^{k+1})/b$, respectively. Take the limit $b \rightarrow 1$ and make back the change $u = \sqrt[k+1]{1-t}$. The functions “ $f_1(a)$ ” and “ $f_2(a)$ ” described in [16, p457] are exactly $J_1(a, b)$ and $J_0(a, b)$ at $b = 1$, respectively. From this point on we shall follow some ideas from [16, p457-9].

The change $t = (1/a - a)u + a$ gives

$$J_1(a, 1) = a^{\frac{1}{k+1}} \int_0^1 \left(\frac{a^{-2} + (a^{-4} - a^{-2})t}{(1-t)t^{2k+1}} \right)^{\frac{1}{2k+2}} dt,$$

and so

$$\frac{\partial J_1(a, 1)}{\partial a} = \frac{J_1(a, 1)}{a(k+1)} + (\text{neg.term}). \quad (32)$$

Moreover, the change $t = au$ for $J_0(a, 1)$ will give

$$\frac{\partial J_0(a, 1)}{\partial a} = \frac{J_0(a, 1)}{a(k+1)} + (\text{pos.term}). \quad (33)$$

Combining (32) with (33) it follows that $J_0(a, 1)/J_1(a, 1)$ is strictly increasing. By taking \mathcal{B} as the beta function, we now closely follow the computations from [16, pp457-8] to conclude that

$$\lim_{a \rightarrow 0} (a^{\frac{1}{k+1}} J_+(a, b)) = 0,$$

$$\lim_{a \rightarrow 0} (a^{\frac{1}{k+1}} J_-(a, b)) = b^{\frac{-k}{k+1}} \mathcal{B}\left(\frac{1}{k+1}, \frac{2k+1}{2k+2}\right),$$

and

$$\lim_{a \rightarrow 0} (a^{\frac{-1}{k+1}} J_0(a, b)) = b^{\frac{k}{k+1}} \mathcal{B}\left(\frac{1}{2k+2}, \frac{2k+3}{2k+2}\right).$$

Namely, for a close to zero one has $J_0 < \cos(\pi/(2k+2)) \cdot J_1$. Up to this point, we have been considering $(a, b) \in (0, 1) \times (a, 1)$. However, the equivalent choice $(b, a) \in (0, 1) \times (0, b)$ will be easier to deal with. Now notice that

$$J_+ \leq (\text{pos.const.}) \int_a^b \frac{(b-t)^{k/(k+1)} dt}{(t-a)^{(2k+1)/(2k+2)},$$

and so the change $t = (b-a)u + a$ gives

$$J_+ \leq (\text{pos.const.}) \int_0^1 \frac{(b-a)^{(2k+1)/(2k+2)} (1-u)^{k/(k+1)} du}{u^{(2k+1)/(2k+2)}} \rightarrow 0, \text{ for } a \rightarrow b.$$

Moreover,

$$J_- \leq (\text{pos.const.}) \int_{1/b}^{1/a} \frac{(1-at)^{-1/(2k+2)} dt}{(bt-1)^{k/(k+1)},$$

and so the change $t = (1/a - 1/b)u + 1/b$ gives

$$J_- \leq (\text{pos.const.}) \int_0^1 \frac{(1/a - 1/b)^{1/(2k+2)} du}{(1-u)^{1/(2k+2)} u^{k/(k+1)}} \rightarrow 0, \text{ for } a \rightarrow b.$$

On the one hand, if $a \rightarrow b$ then J_{\pm} will both vanish. On the other hand, J_0 will remain finite and positive. Therefore $J_0 > \cos(\pi/(2k+2)) \cdot J_1$ when a is close to b . Let us define $\mathcal{D} := \{z \in \mathbb{C} : 0 < \text{Im } z < \text{Re } z < 1\}$. Until this point we have that

There is an analytic curve $\alpha : (0, 1) \rightarrow \mathcal{D}$ for which any $s \in (0, 1)$ will make the choice $(b, a) = \alpha(s)$ a solution for (30). Up to orientation reversing, $\lim_{s \rightarrow 0} \alpha(s) = (0, 0)$ and $\lim_{s \rightarrow 1} \alpha(s) = (1, a_1)$, for some $a_1 \in (0, 1)$. Moreover, when s is sufficiently close to 1, $\alpha(s)$ is a graph of a as a function of b .

From now on we shall always work with $(b, a) = \alpha(s)$, for some $s \in (0, 1)$. For the integrands of (29), make the change $t = \varepsilon u + a$ with $\varepsilon = b - a$. One easily computes

$$\lim_{s \rightarrow 0} \frac{I_0}{\varepsilon^{2k+2}} = \lim_{s \rightarrow 0} \varepsilon^{\frac{2k}{2k+2}} \int_0^1 \left(\frac{t(u)}{(1-at(u))u^{2k+1}} \right)^{1/(2k+2)} \cdot \left(\frac{1-u}{1-bt(u)} \right)^{k/(k+1)} du = 0 \quad (34)$$

and

$$\lim_{s \rightarrow 0} \frac{I_1}{\varepsilon^{2k+2}} = \lim_{s \rightarrow 0} \int_0^1 \frac{[(1-bt(u))/(1-u)]^{k/(k+1)}}{[u(1-at(u))^{2k+1} t(u)^{2k+3}]^{1/(2k+2)}} du = \infty. \quad (35)$$

The careful reader must have noticed that, intuitively, the extreme case $b = 1$ corresponds to the Callahan-Hoffman-Meeks surfaces M_k , described in [3]. Their underlying Riemann surfaces have lower genera, and so it is hard to formalise any convergence statement. However, the Callahan-Hoffman-Meeks surfaces were again described in [16], where the integrals for the period problem coincide with $J_0|_{b=1}$ and $J_1|_{b=1}$. In the case of [16], the integration of $\text{Re}(1/\hat{g} - \hat{g}, i/\hat{g} + i\hat{g}, 2)dh$ along $\delta + \Delta$ is a geodesic in the plane $x_2 = 0$, connecting the saddles $z = a$ and $z = 1/a$, and symmetric under reflection in the plane $x_3 = 1/2$. In [3] those surfaces were proved to be embedded, and therefore the geodesic cannot cross the vertical axis, except at $z = a$ and $z = 1/a$. Hence $\text{Re} \int_{\delta} (1/\hat{g} - \hat{g})dh = I_1|_{b=1} - I_0|_{b=1} < 0$. Together with (34) and (35), this gives $s^* \in (0, 1)$ for which $(b, a) = \alpha(s^*)$ simultaneously solves (29) and (30).

8. Embeddedness of the Hoffman-Wohlgemuth surfaces

In this last section we use arguments very similar to [10, p60-2] or [26, p360-2]. For convenience of the reader, we recall that every $k \in \mathbb{N}^*$ admits a well-defined complete minimal immersion $X : \mathbb{N} \rightarrow \mathbb{R}^3/\mathcal{T}$, where $\mathbb{N} = \overline{\mathbb{N}} \setminus z^{-1}(\{0, \infty\})$,

$$\overline{\mathbb{N}} = \left\{ (z, u) \in \hat{\mathbb{C}} \times \hat{\mathbb{C}} : u^{2(k+1)} = \frac{z(z-a)}{az-1} \cdot \left(\frac{bz-1}{z-b} \right)^2 \right\},$$

and X is given by the Weierstrass pair

$$g = \frac{z}{u^k} \quad \text{and} \quad dh = \frac{ab_0 dz}{\sqrt{z(z-a)(az-1)}}.$$

Here, a and b were determined in the previous section, and $b_0 \in i\mathbb{R}_+^*$ is such that $\int_{-\infty}^0 dh = 1$. Now consider the domain $D := \{z \in \mathbb{C} : |z| < 1 < 1 + \text{Im}(z)\}$. By choosing appropriate logarithm branches, one sees that $g(D)$ is contained in a hemisphere of $\hat{\mathbb{C}}$ (see Figure 10). As before, take $\tilde{g} = e^{-i\pi/(2k+2)}g$ and call $\tilde{X} : \mathbb{N} \rightarrow \mathbb{R}^3/\mathcal{T}$ the minimal immersion given by (\tilde{g}, dh) . If (x_1, x_2, x_3) are the coordinates of \tilde{X} , then $(x_2, x_3) : D \rightarrow \mathbb{R}^2$ is an immersion, and so its image boundary coincides with $(x_2, x_3)(\partial D \setminus \{0\})$.

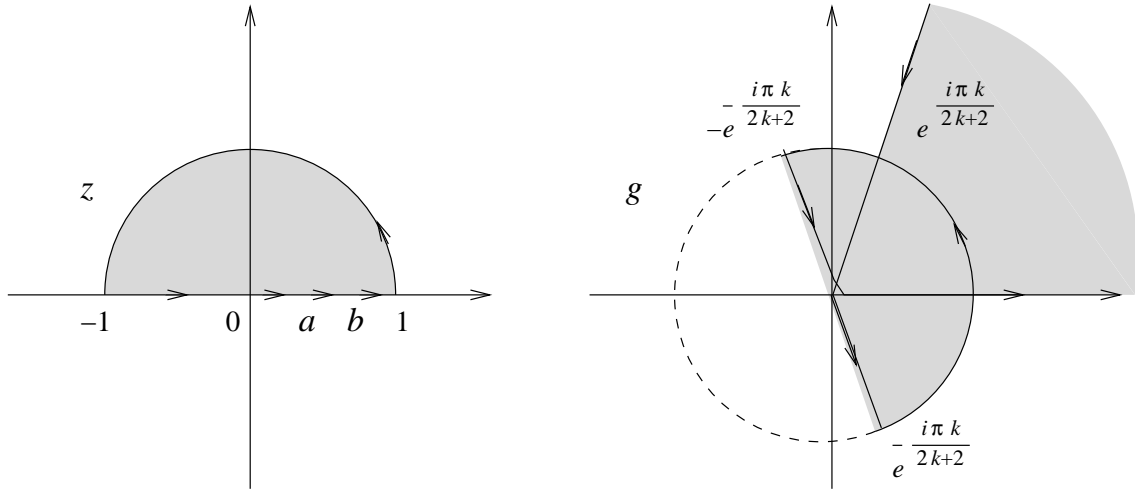


Figure 10: The domain D and its image under g .

Now consider the following stretches of ∂D : $[0, a]$, $[a, b]$, $[b, 1]$, $e^{i[0, \pi]}$, $[-1, 0]$. After analysing dh and \tilde{g} on each of them, we conclude that the projection of $\tilde{X}(\partial D)$ on the plane x_2x_3 , which we call \mathcal{C} , will be a curve like the ones depicted in Figure 11. In fact, this holds for $k > 1$. For $k = 1$, the stretch of \mathcal{C} that connects 0 with a point in Ox_3 is contained in that axis.

Notice that $\tilde{X}(D)$ is contained in its convex hull (see [22] for details), which is a subset of $\mathcal{F} := \{(x_1, x_2, x_3) \in \mathbb{R}^3 : x_2 \geq 0, 0 \leq x_1 \leq x_2 \tan(\pi/(k+1)) \text{ and } 0 \leq x_3 \leq 1/2\}$. Successive reflections in the components of $\partial \mathcal{F}$ will tessellate \mathbb{R}^3/\mathcal{T} in exactly $8k + 8$ congruent pieces. Let \mathcal{F}' be any of these pieces. Of course, $\mathcal{F}' \supset \tilde{X}(\partial D \setminus \{0\})$, this one all made up by symmetry

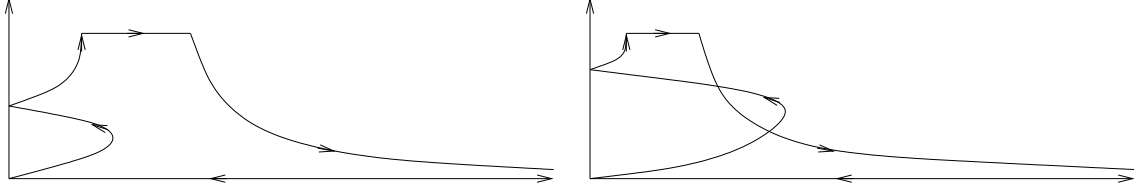


Figure 11: Possible projections of $\tilde{X}(\partial D)$ onto x_2x_3 .

curves and one ray, in such a way that $\tilde{X}(\mathbb{N}) \cap \mathcal{F}' \cong \tilde{X}(\overline{D}^*)$.

From (6), the divisor of g is given by

$$[g] = \frac{p_1^{k+2}(q_2r_1r_3)^k}{p_2^{k+2}(q_1r_2r_4)^k},$$

thus

$$[dg] = \frac{p_1^{k+1}(q_2r_1r_3)^{k-1}}{p_2^{k+3}(q_1r_2r_4)^{k+1}} \cdot D,$$

where D is a divisor with $8k + 8$ zeroes, because $\deg(dg) = -\chi(\overline{\mathbb{N}}) = 8k$. Now, if we had $dg \neq 0$ in D , then $g|_D$ would be an unbranched covering. However, any curve in D connecting 0 and b is taken to a loop with base-point 0. But $g(D)$ is simply connected, hence the pre-image of any loop should be a closed curve. This contradiction implies that dg has at least one zero in D . Now recall that \mathbb{R}^3/\mathcal{T} is tessellated by exactly $8k + 8$ pieces congruent to \mathcal{F} . Consequently, $dg \neq 0$ on $\partial D \setminus \{0, b\}$, and therefore \mathcal{C} is a monotone curve. In particular, all of its stretches depicted in Figure 11 are convex.

Since $(x_2, x_3) : D \rightarrow \mathbb{R}^2$ is an immersion and also injective on $\partial D \setminus \{0\}$, then it is a covering map. From [10] or [23], the Gaussian curvature of minimal surfaces is given by

$$K = \frac{-16}{(|g| + |g|^{-1})^4} \left| \frac{dg/g}{dh} \right|^2.$$

Since neither g nor dh vanishes on (a, b) , this means that $K \neq 0$ on this stretch. In Figure 11, this means that $(x_2, x_3)(D)$ contains an open neighbourhood at the right-hand side of the corresponding stretch for \mathcal{C} . But $(x_2, x_3) : D \rightarrow \mathbb{R}^2$ is an immersion, which implies that \mathcal{C} must be simple. Therefore, $\text{Int } \mathcal{C}$ is simply connected, and the covering map $(x_2, x_3)|_D$ must be a graph. Consequently, $\tilde{X} : D \rightarrow \mathbb{R}^3/\mathcal{T}$ is an embedded piece, and from the above discussion of \mathcal{F} , $\tilde{X} : \mathbb{N} \rightarrow \mathbb{R}^3/\mathcal{T}$ is an embedding. This concludes the proof of Theorem 1.1.

References

- [1] C.J. Costa, *Uniqueness of minimal surfaces embedded in \mathbb{R}^3 with total curvature 12π* , J. Differential Geom. **30** (1989) 597–618.
- [2] M. Callahan, D. Hoffman & H. Karcher, *A family of singly periodic minimal surfaces invariant under a screw motion*, Experiment. Math. **2** (1993) 157–182.
- [3] M. Callahan, D. Hoffman & W.H. Meeks, *Embedded minimal surfaces with an infinite number of ends*, Invent. Math. **96** (1989) 459–505.
- [4] M. Callahan, D. Hoffman & W.H. Meeks, *The structure of singly-periodic minimal surfaces*, Invent. Math. **99** (1990) 455–481.

- [5] H.I. Choi, W.H. Meeks & B. White, *A rigidity theorem for properly embedded minimal surfaces in \mathbb{R}^3* , J. Differential Geom. **32** (1990) 65–76.
- [6] L. Ferrer & F. Martín, *Minimal surfaces with helicoidal ends*, Math. Z. **250** (2005) 807–839.
- [7] D. Hoffman & H. Karcher, *Complete embedded minimal surfaces of finite total curvature*, Encyclopedia of Math. Sci., Springer Verlag **90** (1997) 5–93.
- [8] D. Hoffman, H. Karcher & F. Wei, *The singly periodic genus-one helicoid*, Comment. Math. Helv. **74** (1999) 248–279.
- [9] D. Hoffman & W.H. Meeks, *Embedded minimal surfaces of finite topology*, Ann. of Math. **131** (1990) 1–34.
- [10] H. Karcher, *Construction of minimal surfaces*, Surveys in Geometry, University of Tokyo (1989) 1–96 and Lecture Notes **12** (1989), SFB256, Bonn.
- [11] N. Kapouleas, *Complete embedded minimal surfaces of finite total curvature*, J. Differential Geom. **47** (1997) 95–169.
- [12] L. Lazard-Holly & W.H. Meeks, *Classification of doubly-periodic minimal surfaces of genus zero*, Invent. Math. **143** (2001) 1–27.
- [13] F.J. López & F. Martín, *Complete minimal surfaces in \mathbb{R}^3* , Publ. Mat. **43** (1999) 341–449.
- [14] F.J. López & A. Ros, *On embedded complete minimal surfaces of genus zero*, J. Differential Geometry **33** (1991) 293–300.
- [15] F. Martín, *A note on the uniqueness of the periodic Callahan-Hoffman-Meeks surfaces in terms of their symmetries*, Geom. Dedicata **86** (2001) 185–190.
- [16] F. Martín & D. Rodríguez, *A characterization of the periodic Callahan-Hoffman-Meeks surfaces in terms of their symmetries*, Duke Math. J. **89** (1997) 445–463.
- [17] F. Martín & M. Weber, *On properly embedded minimal surfaces with three ends*, Duke Math. J. **107** (2001), 533–559.
- [18] W.S. Massey, *Algebraic topology: an introduction*, Graduate Texts in Mathematics, Springer, New York (1967).
- [19] W.H. Meeks, J. Pérez & A. Ros, *Uniqueness of the Riemann minimal examples*, Invent. Math. **131** (1998) 107–132.
- [20] W.H. Meeks & H. Rosenberg, *The uniqueness of the helicoid*, Ann. of Math. **161** (2005) 727–758.
- [21] J.C.C. Nitsche, *Lectures on minimal surfaces*, Cambridge University Press, Cambridge (1989).
- [22] R. Osserman, *The convex hull property of immersed manifolds*, J. Differential Geometry **6** (1971/72) 267–270.
- [23] R. Osserman, *A survey of minimal surfaces*, Dover, New York, 2nd ed (1986).
- [24] J. Pérez, M. Rodríguez & M. Traizet, *The classification of doubly periodic minimal tori with parallel ends*, J. Differential Geom. **69** (2005) 523–577.
- [25] J. Pérez & M. Traizet, *The classification of singly periodic minimal surfaces with genus zero and Scherk type ends*, Trans. Amer. Math. Soc. (to appear).
- [26] V. Ramos Batista, *A family of triply periodic Costa surfaces*, Pacific J. Math. **212** (2003) 347–370.
- [27] V. Ramos Batista, *Noncongruent minimal surfaces with the same symmetries and conformal structure*, Tohoku Math. J. **56** (2004) 237–254.
- [28] R. Schoen, *Uniqueness, symmetry and embeddedness of minimal surfaces*, J. Differential Geom. **18** (1983) 701–809.
- [29] M. Traizet, *An embedded minimal surface with no symmetries*, J. Differential Geom.

60 (2002) 103–153.

- [30] M. Weber, *A Teichmüller theoretical construction of high genus singly periodic minimal surfaces invariant under a translation*, *Manuscripta Math.* **101** (2000) 125–142.
- [31] M. Wohlgemuth, *Minimal surfaces of higher genus with finite total curvature*, *Arch. Rational Mech. Anal.* **137** (1997) 1–25.

IME - UNIVERSITY OF SÃO PAULO
RUA DO MATÃO 1010
05508-090, SÃO PAULO - SP, BRAZIL
E-mail address: paqs@ime.usp.br

CMCC - ABC FEDERAL UNIVERSITY
RUA CATEQUESE 242, 3rd FLOOR
09090-400, SANTO ANDRÉ - SP, BRAZIL
E-mail address: valerio.batista@ufabc.edu.br